The Plant Cell, Vol. 26: 3272–3285, August 2014, www.plantcell.org

Analysis of Natural and Induced Variation in Tomato Glandular Trichome Flavonoids Identifies a Gene Not Present in the Reference Genome[W][OPEN]

Jeongwoon Kim,[a,b] Yuki Matsuba,[c] Jing Ning,[d] Anthony L. Schilmiller,[d] Dagan Hammar,[c] A. Daniel Jones,[d,e] Eran Pichersky,[c] and Robert L. Last[a,d,1]

[a] Department of Plant Biology, Michigan State University, East Lansing, Michigan 48824
[b] Department of Energy Plant Research Laboratory, Michigan State University, East Lansing, Michigan 48824
[c] Department of Molecular, Cellular, and Developmental Biology, University of Michigan, Ann Arbor, Michigan 48109
[d] Department of Biochemistry and Molecular Biology, Michigan State University, East Lansing, Michigan 48824
[e] Department of Chemistry, Michigan State University, East Lansing, Michigan 48824

ORCID ID: 0000-0001-6974-9587 (R.L.L.)

Flavonoids are ubiquitous plant aromatic specialized metabolites found in a variety of cell types and organs. Methylated flavonoids are detected in secreting glandular trichomes of various *Solanum* species, including the cultivated tomato (*Solanum lycopersicum*). Inspection of the sequenced *S. lycopersicum* Heinz 1706 reference genome revealed a close homolog of *Solanum habrochaites* MOMT1 3′/5′ myricetin *O*-methyltransferase gene, but this gene (Solyc06g083450) is missing the first exon, raising the question of whether cultivated tomato has a distinct 3′ or 3′/5′ *O*-methyltransferase. A combination of mining genome and cDNA sequences from wild tomato species and *S. lycopersicum* cultivar M82 led to the identification of Sl-MOMT4 as a 3′ *O*-methyltransferase. In parallel, three independent ethyl methanesulfonate mutants in the *S. lycopersicum* cultivar M82 background were identified as having reduced amounts of di- and trimethylated myricetins and increased monomethylated myricetin. Consistent with the hypothesis that Sl-*MOMT4* is a 3′ *O*-methyltransferase gene, all three myricetin methylation defective mutants were found to have defects in *MOMT4* sequence, transcript accumulation, or 3′-*O*-methyltransferase enzyme activity. Surprisingly, no *MOMT4* sequence is found in the Heinz 1706 reference genome sequence, and this cultivar accumulates 3-methyl myricetin and is deficient in 3′-methyl myricetins, demonstrating variation in this gene among cultivated tomato varieties.

INTRODUCTION

It is estimated that there are hundreds of thousands of metabolites produced by plants (Pichersky and Lewinsohn, 2011). Because they are structurally diverse and taxonomically restricted, understanding the evolution of the metabolic networks that produce these compounds is especially interesting. Many enzymes of specialized metabolism diversify more rapidly than those of central metabolism (Chae et al., 2014) and are not often found in reference organisms such as *Arabidopsis thaliana*, rice (*Oryza sativa*), and maize (*Zea mays*). These characteristics create challenges for characterizing the genes and enzymes that produce these interesting compounds (Schilmiller et al., 2012a; Winzer et al., 2012). Furthermore, the portion of the coding region of the genome devoted to the genes encoding these enzymes and their regulators is substantial (estimated at 10 to 20% of total genes; Somerville and Somerville, 1999). This, combined with their rapid diversification, which includes both small changes in nucleotide sequences as well as large duplications and deletions, often creates difficulties for disciplines dependent on interpretations of differences in DNA sequences between individuals and species, such as ecology and evolutionary biology.

Secretory glandular trichomes (referred to as "trichomes" below) are produced on the surfaces of varied plant species and organs, and these structures accumulate a wide variety of plant specialized metabolites (Wagner, 1991; Schilmiller et al., 2008; Glas et al., 2012; Kim et al., 2012; Tissier, 2012; Lange and Turner, 2013). Many of these chemical compounds protect plants from herbivorous insects (Kang et al., 2010a, 2010b, 2014; Weinhold and Baldwin, 2011). Furthermore, some trichome metabolites contribute to food flavor and aroma, for example, in mint (*Mentha* spp), basil (*Ocimum basilicum*), and hops (*Humulus lupulus*; Gang, 2005; Wang et al., 2008), or are used as therapeutic drugs including cannabinoids and artemisinin (Furr and Mahlberg, 1980; Klein, 2005; Liu et al., 2011). Because they protrude from the epidermis and are accessible for study, trichome metabolites and metabolic pathways have been intensively studied in various plants (Schilmiller et al., 2008).

Flavonoids are structurally diverse nonvolatile plant specialized metabolites and include chalcones, flavanones, flavones, flavonols, and anthocyanins (Buer et al., 2010). Flavonols, a subclass of flavonoids, include kaempferol, quercetin, and myricetin (the structure of myricetin is shown in Figure 1) and are relatively widespread and

[1] Address correspondence to lastr@msu.edu.
The author responsible for distribution of materials integral to the findings presented in this article in accordance with the policy described in the Instructions for Authors (www.plantcell.org) is: Robert L. Last (lastr@msu.edu).
[W] Online version contains Web-only data.
[OPEN] Articles can be viewed online without a subscription.
www.plantcell.org/cgi/doi/10.1105/tpc.114.129460

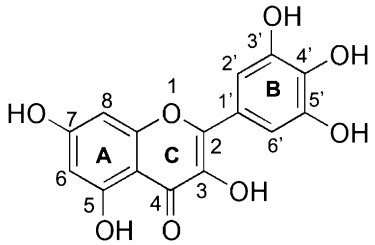

Figure 1. The Structure of the Flavonol Myricetin.

The structure is shown with the numbering system indicated. The hydroxyl groups of myricetin are typically modified in vivo, for example, by methylation or glycosylation.

abundant in plants (Herrmann, 1976). Flavonols are typically found as modified compounds, with glycosylation and methylation of the various hydroxyl groups commonly observed (Stevens et al., 1995; Braca et al., 2001; Schilmiller et al., 2010a; McDowell et al., 2011; Schmidt et al., 2011). Chemical modifications are known to affect the physical properties and chemical reactivity of flavonoids. For instance, *O*-methylation of hydroxyl groups makes the compounds more hydrophobic, while glycosylation increases their hydrophilicity (Heim et al., 2002).

Plants contain little, if any, nonmodified myricetin (reviewed in Schmidt et al., 2011; Schmidt et al., 2012). Nonglycosylated myricetin is always methylated at the 3-hydroxyl (-OH) position (Figure 1) and may be methylated at other hydroxyl positions as well. We recently showed that the trichomes of the wild tomato species *Solanum habrochaites* accession LA1777 synthesize and store myricetin derivatives that are all methylated at the 3-hydroxyl position and some are additionally methylated at one or more of the 3′, 4′, 5′, and 7 hydroxyl positions (Schmidt et al., 2011, 2012).

Three trichome-active myricetin *O*-methyltransferases (MOMTs) were identified from *S. habrochaites*. The first two, *MOMT1* and *MOMT2*, are 3′/5′ and 4′/7 *O*-methyltransferases, respectively (Schmidt et al., 2011, 2012). The Sh-*MOMT3* gene encodes myricetin 3 *O*-methyltransferase, the enzyme that methylates the 3 position of myricetin (Schmidt et al., 2012). The cultivated tomato *Solanum lycopersicum* enzymes encoded by the apparent orthologs of Sh-*MOMT2* and *MOMT3* were partially characterized biochemically and shown to have activity similar to that of the corresponding *S. habrochaites* enzymes (Schmidt et al., 2011, 2012), but surprisingly the *MOMT1* gene of cultivated tomato has a deletion of its first exon and therefore appears not to encode a functional enzyme (Schmidt et al., 2012). This raised the question of whether tomato has an *O*-methyltransferase (OMT) with myricetin 3′ or 3′/5′ methylation activity as previously reported in other plant species (Muzac et al., 2000; Kim et al., 2006). However, no strong candidate gene was found in the *S. lycopersicum* Heinz 1706 reference genome sequence (Supplemental Table 1).

Forward genetic phenotypic screens of natural variants and of populations containing induced mutations provide a powerful approach to discover genes that affect biological processes. This approach is especially useful for identifying genes whose functions cannot be inferred based upon homology to characterized gene products or genes not represented in EST collections or included in genome assemblies. Genetic screening for changes in metabolite profiles using mass spectrometry-based analytical chemical approaches is an especially powerful way to dissect metabolic pathways (Last et al., 2007). Cultivated tomato is a good system for such forward genetic screens because induced mutant populations and chromosomal substitution lines such as introgression lines (ILs) are available (Eshed and Zamir, 1994; Menda et al., 2004).

In this study, liquid chromatography-mass spectrometry-based chemical analysis of *S. lycopersicum* M82 tomato trichomes showed that they contain 3,3′-dimethylmyricetin and 3,3′,7-trimethylmyricetin as well as 3-monomethylmyricetin, indicating that this cultivar must have 3′ MOMT activity (but no 5′ MOMT activity). Analysis of randomly generated tomato ethyl methanesulfonate (EMS) mutants and *S. lycopersicum* M82 × *Solanum pennellii* LA0716 ILs indicated that genes on the bottom of chromosome 6 influence trichome myricetin methylation. Three independent M82 EMS mutants with increased 3-methyl myricetin and undetectable 3,3′-dimethylated and 3,3′,7-trimethylated myricetins were among the phenotypic variants discovered. These mutants were demonstrated to have defects in Sl-*MOMT4*, a trichome-expressed gene on chromosome 6 encoding a flavonoid *O*-methyltransferase that is absent from the *S. lycopersicum* Heinz 1706 variety genome assembly (Tomato Genome Consortium, 2012). The M82 wild-type Sl-MOMT4 enzyme was found to methylate myricetin at the 3′ position, while plants carrying the mutant alleles either showed low trichome *MOMT4* transcript levels and/or the purified protein had decreased in vitro 3′-*O*-methyltransferase activity. The discovery of the *S. lycopersicum* M82 *MOMT4* gene and its effect on modification of flavonols in trichomes demonstrates the power of combining classical mutation screening with large-scale metabolic profiling in a plant genus for which extensive genomic and transcriptomic sequences are available. This work further demonstrates how variable and labile pathways of *Solanum* trichome specialized metabolism are within the same genus and even the same species.

RESULTS

Identification and Characterization of Sl-*MOMT4* as a 3′ Myricetin *O*-Methyltransferase

Analysis of specialized metabolites in trichomes of the *S. lycopersicum* M82 cultivar revealed the presence of a mixture of monomethylated, dimethylated, and trimethylated myricetins (3-, 3,3′-, and 3,3′,7-methylmyricetins, respectively; Figures 2 and 3). This chemical phenotype is consistent with the existence of a MOMT activity in M82 trichomes.

Two lines of reasoning focused our bioinformatics search for candidate genes to the bottom of chromosome 6. First, multiple MOMT genes had been found on tomato chromosome 6 (Schmidt et al., 2012). Second, results of screening of trichome metabolite diversity in *S. lycopersicum* × *S. pennellii* ILs (Schilmiller et al., 2010a) revealed a shift of methylated myricetin accumulation toward more highly methylated myricetins in both IL6-3 and IL6-4 lines. Profiles using positive mode liquid chromatography-mass spectrometry showed these two ILs predominately accumulated tri(3,3′,7)- and tetra(3,3′,5′,7)-methylated myricetins,

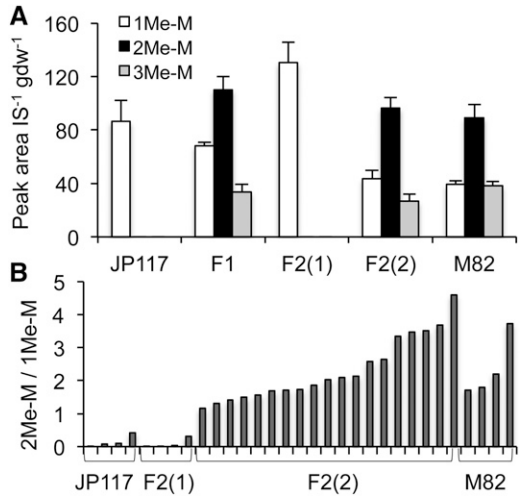

Figure 2. Results of Negative-Mode LC-ToF-MS Analysis of Methylated Myricetin Phenotypes.

(A) Me-M profiles in leaf dips of JP117, M82 × JP117 backcross F1 and F2 plants, and M82. Of 23 backcross F2 plants, four are labeled as F2 (1), while 19 are labeled as F2 (2). The grouping of BC F2 plants was based on the individual chemical profiles from **(B)**. Four replicate plants were assayed for each genotype, except F2 plants. The averaged values are presented with standard errors in the graphs. 1Me-M, 2Me-M, and 3Me-M indicates mono-, di-, and tri-Me-M respectively. An identical nomenclature system is used in subsequent figures, unless specified otherwise. **(B)** The ratio of di- to mono-Me-M (2Me-M/1Me-M) is shown for individual F2 plants tested in **(A)**.

whereas di(3,3′)-methylated myricetin was dominant in M82 *S. lycopersicum* (Figure 3; Supplemental Figure 1). Because IL6-4 is completely contained within IL6-3 on the bottom of chromosome 6, these results suggested that the chemical phenotypes were associated with this relatively small chromosomal location.

Detailed analysis of the Heinz 1706 cultivar tomato genome sequence revealed that this chromosomal location contains Sl-*MOMT1* (the presumptive ortholog of Sh-*MOMT1*, the gene encoding the 3′/5-MOMT from *S. habrochaites*). However, as described by Schmidt et al. (2012), Sl-*MOMT1* in the tomato Heinz 1706 genome sequence has a deletion of the first exon, including the Met start codon, and is therefore likely to be nonfunctional. We amplified and sequenced this region from the M82 cultivar and the sequence was identical to that of the reference Heinz 1706 genome, with its *MOMT1* missing the first exon. The Heinz sequence in the IL6-4 region revealed an intact Sl-*MOMT3* gene (the apparent ortholog of Sh-*MOMT3*, the gene encoding the 3-MOMT from *S. habrochaites*). Furthermore, Sl-*MOMT2a* and Sl-*MOMT2b*, the apparent orthologs of Sh-*MOMT2*, and the gene encoding the 7/4'-MOMT from *S. habrochaites* are found to be outside of this region on chromosome 6 (Schmidt et al., 2012; Supplemental Figure 2). No other genes with homology to OMTs were found in the Heinz 1706 IL 6-4 region.

The lack of a strong OMT candidate gene at the bottom of chromosome 6 led us to consider the possibility that the tomato genome sequence assembly might be incomplete, as seen for the terpene synthase gene cluster on chromosome 8 (Falara et al., 2011), or that additional MOMT genes are found in the M82 genome compared with the Heinz genome. Additional OMT sequences for tomato were sought by BLAST analysis with shotgun DNA sequence of two wild species of tomato, *S. pennellii* (Bolger et al., 2014) and *S. pimpinellifolium* (http://solgenomics.net/tools/blast/index.pl), and trichome EST libraries (http://bioinfo.bch.msu.edu/trichome_est; Schilmiller et al., 2010b; McDowell et al., 2011). Two short contigs in the genome sequence of *S. pennellii* were found to carry genes with high similarity to Sh-*MOMT1* and Sl-*MOMT1*. The first contig contains a nearly complete sequence of a gene missing only the beginning of exon 1, and the sequence was completed using an EST. This completed sequence was determined to be the presumptive ortholog of Sl-*MOMT1* in part due to extensive 3′ noncoding sequence similarity to Sh-*MOMT1* and Sl-*MOMT1* (Figure 4; Supplemental Data Set 1). The second smaller fragment contained a gene encoding a very similar but not identical protein, which we named Sp-*MOMT4* (Figure 4; Supplemental Data Set 1 and Supplemental Figure 3). A similar sequence, Spm-*MOMT4* (Figure 4; Supplemental Data Set 1 online), was also found on a small fragment from the genome of *S. pimpinellifolium*, which is closely related to cultivated tomato (Rodriguez et al., 2009).

The sequences of Sp-*MOMT4* and Spm-*MOMT4* were used to design oligonucleotide primers to amplify the complete gene sequence from M82 genomic DNA as well as to obtain a complete cDNA sequence (Figure 4; Supplemental Figure 3). The gene sequence was also amplified from IL6-3 and IL6-4 and found to be identical to Sp-*MOMT4* (with one nucleotide substitution in the second intron), indicating that the gene maps to the end of chromosome 6 (Supplemental Figure 3). To test the hypothesis that Sl-*MOMT4* is involved in trichome methylated myricetin metabolism, trichome gene expression of Sl-*MOMT4* was investigated. Higher levels of *MOMT4* transcript accumulation were observed in isolated stem and petiole trichomes of wild-type tomato M82 plants than in whole stem and petiole with or without trichomes (Figure 5; compare "T," isolated trichomes, to "W," whole stems and petioles). Taken together, these cDNA, genomic DNA, and expression analyses identified a trichome-expressed MOMT homolog on the bottom of

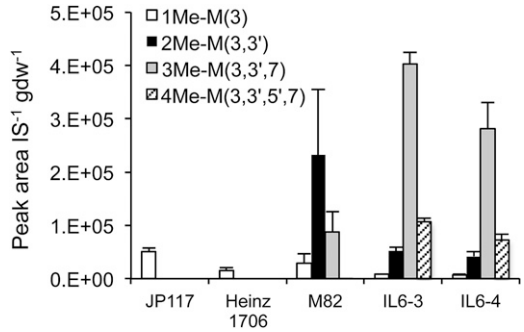

Figure 3. Positive Mode LC-MS/MS Analysis of Methyl-Myricetin Phenotypes.

Relative amounts of the various methyl-myricetin isomers from leaf dips are shown for JP117, Heinz 1706, M82, IL6-3, and IL6-4. Three to six replicate plants were assayed for each genotype. The averaged values are presented with standard errors in the graph.

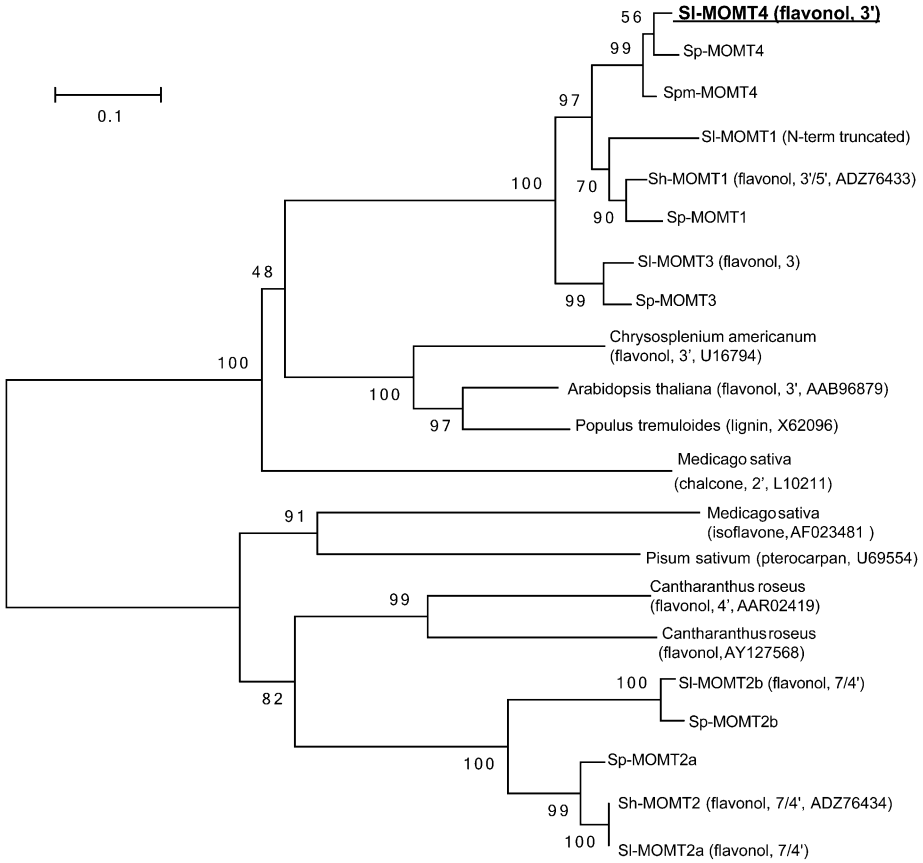

Figure 4. Evolutionary Relationships of *S. lycopersicum* MOMT4 to Selected Plant OMTs.

Protein sequence was obtained for previously characterized plant OMTs. Information is presented for individual OMTs including the name of the plant species from which the OMT was characterized, their annotated substrate identified from biochemical experiments, and accession number of the protein sequence. Bootstrap test results with $n = 1000$ is shown next to each branch. Sp, Sl, Spm, and Sh indicate *S. pennellii*, *S. lycopersicum*, *S. pimpinellifolium*, and *S. habrochaites*, respectively.

S. lycopersicum M82 chromosome 6, which we named Sl-*MOMT4.*

To test for the activity of the protein encoded by Sl-*MOMT4*, we expressed wild-type M82 Sl-*MOMT4* cDNA in *Escherichia coli* and tested the protein for OMT activity with myricetin as substrate. The enzyme converted myricetin to monomethylated myricetin, as demonstrated by liquid chromatography negative ion mode time-of-flight mass spectrometry (LC-ToF-MS) (Figures 6A and 6B). Neither di- nor trimethylated myricetin product was detected from the assays. This reaction product was further analyzed by the liquid chromatography-positive ion mode tandem mass spectrometry (MS/MS) method (Schmidt et al., 2011; Li et al., 2013) to obtain structural information and the result confirmed it as 3′-methyl myricetin (see the structure in Figure 6B; Supplemental Figure 4), revealing that Sl-MOMT4 is a 3′-MOMT. Next, we investigated OMT activities of Sl-MOMT4 enzyme with myricetin, 3′-methylmyricetin, or 3′,5′-dimethylmyricetin as substrates together with nonsaturating levels of [methyl-^{14}C] *S*-adenosyl-L-methionine (SAM) as the methyl donor. At a concentration of 0.2 mM of the flavonoid substrates and 1.7 μM [methyl-^{14}C]-SAM, the 5′-OMT activity of Sl-MOMT4 on 3′-methylmyricetin was only 2.6% of its 3′-OMT activity with myricetin. In comparison, Sh-MOMT1 had 65% 5′-OMT activity with 3′-methylmyricetin compared with its 3′-OMT activity with myricetin, which was consistent with previous reported results (Schmidt et al., 2011). Neither enzyme had activity on 3′,5′-dimethyl myricetin.

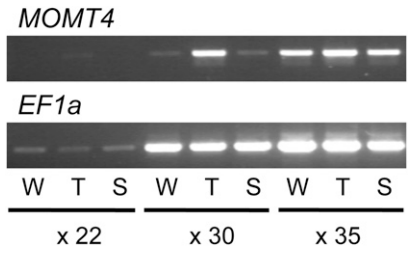

Figure 5. *MOMT4* Is Expressed in Trichomes.

RT-PCR results revealed expression of *MOMT4* in trichomes. M82 total RNA was isolated from whole stem and petiole (W), isolated total stem and petiole trichomes (T), and stem and petiole without trichomes (S). PCR was performed with 22, 30, and 35 cycles.

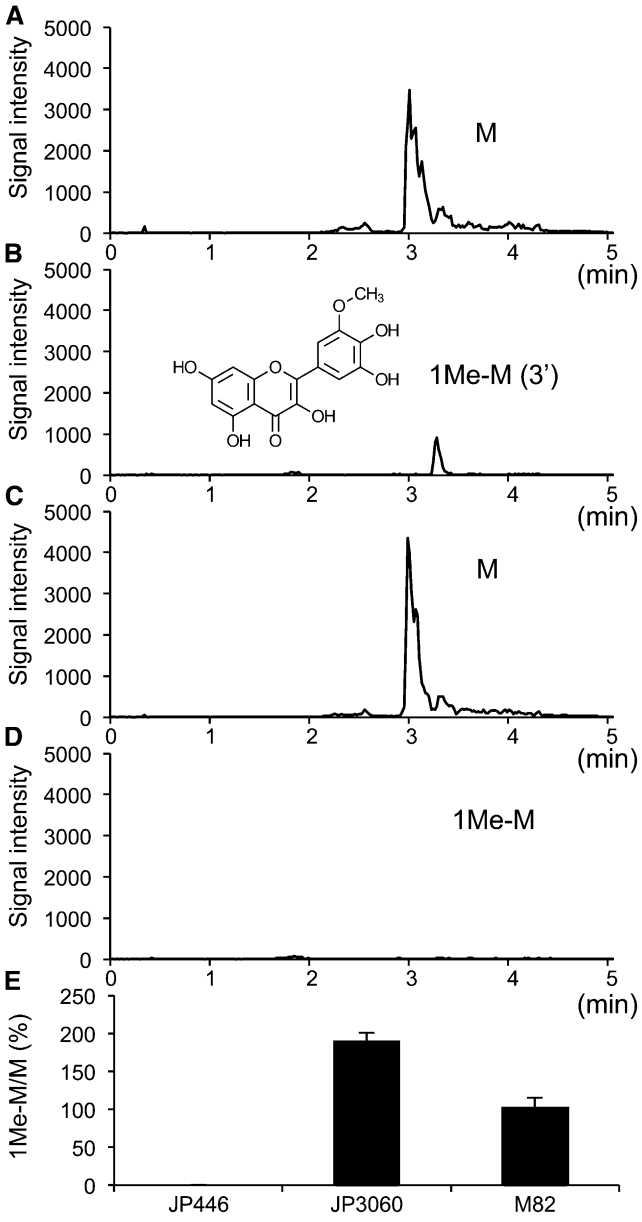

Figure 6. Recombinant Sl-MOMT4 Enzyme Activity.

(A) to **(D)** Extracted ion chromatograms (XICs) for myricetin and monomethylated myricetin are shown. XICs for myricetin substrate with m/z 317 (**[A]** and **[C]**). XICs for monomethylated myricetin product with m/z 331 (**[B]** and **[D]**). With M82 wild-type MOMT4 enzyme (**[A]** and **[B]**) and with no recombinant protein (**[C]** and **[D]**). The structure of 3′-*O*-methyl myricetin is shown (see Supplemental Figure 4 for details). Three replicates were tested in this assay with or without M82 MOMT4, and all exhibited consistent results as presented.

(E) Enzyme activity calculated as the ratio of monomethylated myricetin product to myricetin substrate (1Me-M/M) and presented relative to M82. Three replicates were tested in each assay, and means ± standard errors are presented.

It was previously concluded that the order of methylation of myricetin in *S. habrochaites* was first at the 3 hydroxyl position, then 3′ and 7 (with the exact order unresolved), followed by 5′ and then 4′ (Schmidt et al., 2011, 2012). The observation that MOMT4 mutants accumulate 3-monomethyl myricetin and not 3,7-dimethyl myricetin (see below) suggests that the methylation of the 3′ hydroxyl precedes the methylation of the 7 hydroxyl.

Identification and Phenotypic Characterization of EMS Mutants with Altered Methylated Myricetin Profiles

A cultivated tomato (*S. lycopersicum* cultivar M82) EMS mutant population of M2 families (Menda et al., 2004) was screened for changes in trichome metabolites by LC-ToF-MS (see Methods for details). The largest class of mutants confirmed in M3 progeny tests has increased ratios of mono- to dimethyl myricetin. Seven such mutants were identified, including JP117, JP130, JP256, JP334, JP446, JP3045, and JP3060 (Supplemental Table 2), and line JP117 was chosen for detailed analysis of phenotype and genetic inheritance. In contrast to M82, which accumulates mono-, di-, and trimethyl myricetins, the JP117 mutant accumulates monomethyl myricetin, with no evidence of accumulation of di- and trimethyl myricetins (Figure 2A). The total summed peak intensity for methylated myricetins was also significantly decreased in the JP117 mutant (~65% of M82, P value < 0.0005 from Student's *t* test).

While the negative mode LC-ToF-MS analysis allows rapid and reproducible high-throughput screening of a broad range of metabolites, it provides limited structural information. Thus, we measured methylated flavonoids in leaf dip extracts by positive mode liquid chromatography-tandem mass spectrometry (LC-MS/MS) using recently described methods (Schmidt et al., 2011; Li et al., 2013). Results were obtained that were qualitatively similar to the negative mode ToF method: Dimethylated myricetin was the most abundant in M82 and the JP117 mutant revealed monomethylated myricetin with neither di- nor trimethylated myricetins detected (Figure 3). Disparities in relative peak intensities seen in the two mass spectrometry methods (compared with M82 in Figures 2A and 3) reflect differences in the ease of ionization and detector characteristics in these instruments. The positive ion mode LC-MS/MS analysis identified positions of the methyl groups on myricetin; namely, 3-methyl myricetin, 3,3′-methyl myricetin, and 3,3′,7-methyl myricetin for mono-, di-, and trimethyl myricetin, respectively (Figure 3; Supplemental Figure 1). Taken together with LC-ToF-MS negative mode analysis results, these results led to the hypothesis that the mutant is defective in a flavonoid 3′ *O*-methyltransferase and prompted further analysis of JP117.

JP117 Is a Recessive Mutation That Maps to the Bottom of Chromosome 6

An M4 line was backcrossed to the parental M82 wild type to generate backcross F1 progeny plants. These were analyzed by negative ion mode LC-ToF-MS and the methylated myricetin profiles compared with those of JP117 and M82. As expected for a loss-of-function mutation, 3,3′-methyl myricetin accumulation was restored in backcross F1 plants (Figure 2A). These results are

consistent with the hypothesis that the JP117 mutation is recessive to the wild type.

Backcross F2 progeny, derived by self-crossing the backcross F1 line, were analyzed to test whether the JP117 mutation segregates as a monogenic Mendelian trait. The ratio of 3,3′-methyl myricetin to 3-methyl myricetin (2Me-M/1Me-M) was used as a diagnostic phenotype (Figure 2B). Of 23 backcross F2 plants, 19 (83%) showed profiles similar to M82, accumulating 3,3′-methyl myricetin as the most abundant compound [F2(2) in Figure 2], while four samples (17%) resembled the JP117 mutant [F2(1) in Figure 2]. χ^2 analysis revealed that these numbers fit the segregation ratio expected for a monogenic Mendelian trait at P = 0.05. These results are consistent with the hypothesis that the JP117 mutation is recessive and segregates as a monogenic recessive trait.

Genetic mapping was performed to localize the causative mutation (Jander et al., 2002). Because the genetic diversity of *S. lycopersicum* is relatively low (Rodriguez-Saona et al., 2011), a polymorphic mapping population was obtained by crossing JP117 to the wild species *S. pennellii* accession LA0716. *S. pennellii* LA0716 was chosen because it is sexually compatible with the cultivated tomato and there are many DNA polymorphisms characterized between the two species. Chemical profiles were analyzed by LC-ToF-MS for 289 F2 plants derived by self-pollination of the outcross (OC) F1 plants (labeled "OC F2" in Supplemental Figure 5A) and compared with those of JP117 and M82. As expected for an interspecific cross, the ratio of 3,3′-methyl myricetin to 3-methyl myricetin was highly variable in the OC F2 mapping population, ranging from 0.09 to 203.97 (corresponding to −1.05 and 2.31 on the $\log_{10}$ scale in Supplemental Figure 5A). The highest ratio among the JP117 mutant control plant extracts (0.60, which is −0.22 on the $\log_{10}$ scale in Supplemental Figure 5A) was used as a cutoff to identify 30 OC F2 plants presumed to be homozygous mutant, and these were used for genetic mapping (Supplemental Figure 5A).

First-pass mapping results with genetic markers throughout the *S. lycopersicum* genome (Sol Genomics Network, http://solgenomics.net/) indicated that the JP117 mutation is on chromosome 6. Fine mapping was performed with polymorphic genetic markers throughout chromosome 6 from the Sol Genomics Network and others generated in this study (Supplemental Figure 5B). All 30 F2 plants revealed *S. lycopersicum* homozygous genotypes with markers 10 through 13, indicating that the JP117 mutation is closely linked to these markers (Supplemental Figure 5B and Supplemental Table 3). The physical locations of marker 9 and the end of chromosome 6 are known to be at 44.58 and 46.04 Mbp, respectively, based on the *S. lycopersicum* reference genome assembly generated using the Heinz 1706 variety (Tomato Genome Consortium, 2012; http://solgenomics.net, SL2.31 chromosome sequence; Supplemental Figure 5B). Taken together, these genetic mapping results indicate that the JP117 allele is located within the last 1.5 Mbp at the bottom of chromosome 6, which is consistent with the hypothesis that it is within the IL6-4 region.

Sl-MOMT4 Is Defective in the High Monomethylated Myricetin EMS Mutants

Mapping of the JP117 high 3-methyl myricetin mutation to the IL6-4 region, which contains *MOMT4*, led us to analyze this gene in the JP117, JP446, and JP3060 mutants. These mutants were chosen because they were found in three different M2 families and thus contain independently derived mutations (Supplemental Table 2). Quantitative RT-PCR analysis of *S. lycopersicum MOMT4* transcripts from the mutant lines (Figure 7) revealed that two of the three mutants, JP117 and JP3060, had almost undetectable transcript levels. In contrast, JP446 mRNA accumulated to nearly wild-type levels.

In addition to being unable to amplify *MOMT4* transcripts from JP117, *MOMT4* genomic DNA sequences could not be amplified from JP117 using two sets of primer combinations derived from different parts of the gene, suggesting that part or all of this gene is missing in this mutant line (Figure 8). The inability to amplify *MOMT4* sequences in JP117 left some doubt as to the nature of the defect in this gene in this mutant line. An allelism test was performed to determine whether the mutant phenotype of JP446 and JP117 results from defect in the same gene. F1 progeny were obtained when JP117 and JP446 mutant plants were crossed in a reciprocal manner and the progeny plants were analyzed for their genotypes and metabolite profiles (see Methods for details). The results showed that these recessive alleles failed to complement in the F1 plants, consistent with the hypothesis that the mutants are defective in the same gene (Supplemental Figure 6).

Sl-*MOMT4* cDNA sequence analysis revealed altered predicted protein coding sequence in mutants JP446 and JP3060 (Figure 9). Both mutants showed G:C to T:A mutations at different positions in the *MOMT4* sequence. JP3060 *MOMT4* has a G:C to T:A mutation at position 967 (Supplemental Figure 3), predicted to cause a change from arginine to histidine at amino acid 323 (Figure 9), adjacent to the conserved protein motif GlyGlyLysGluArgThr in OMTs (Ibrahim et al., 1998). JP446 *MOMT4* also has a G:C to T:A mutation at position 688 of *MOMT4* (Supplemental Figure 3), predicted to change leucine to isoleucine at amino acid 230 (Figure 9). This amino acid is located in the protein motif GlyIleAsnPheAspLeuProHisVal conserved among previously characterized plant OMTs (Ibrahim et al., 1998).

To test whether the MOMT mutants have differential enzyme activities, assays were performed with the identical amount of purified MOMT protein variants and incubation time. No myricetin

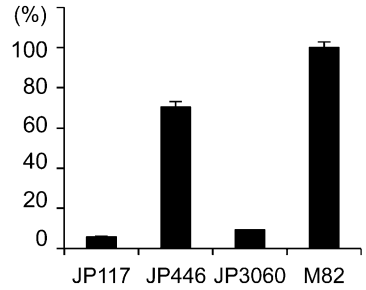

Figure 7. *MOMT4* mRNA Accumulation Is Low in JP117 and JP3060 Mutant Trichomes.

This quantitative RT-PCR analysis was performed using total RNA from stem and petiole trichomes pooled from eight plants for each genotype and repeated three times. Average with SE is presented.

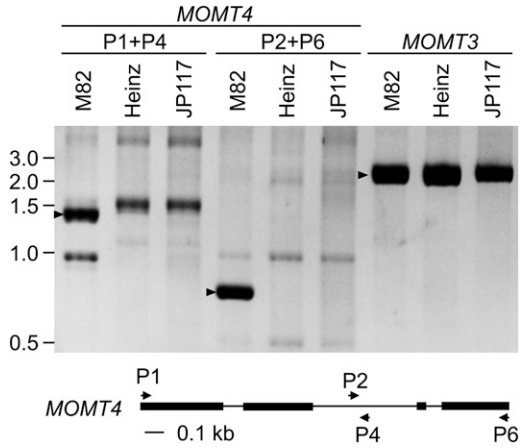

Figure 8. Genomic PCR Analysis of *MOMT4* and *MOMT3* in *S. lycopersicum* M82, Heinz 1706, and JP117.

Two pairs of primers, P1+P4 and P2+P6, were used for *MOMT4*. The positions of the primers are shown compared with *MOMT4* gene sequence with exons bold lines and introns thinner lines. *MOMT3* was amplified as a control. The expected sizes of PCR products are indicated with arrowheads, and they were verified by sequencing. Other amplified fragments present in the lanes of *MOMT4* amplification but unmarked by arrows were also sequenced and determined not from *MOMT4*. See Supplemental Table 5 for the primer sequences.

methylation was observed when the MOMT4 protein from mutant JP446 was tested in vitro, where M82 wild-type MOMT4 produced 3′-methyl myricetin (Figure 6E). These results are consistent with the hypothesis that defective enzyme activity causes the mutant phenotype. Unlike JP446, MOMT4 protein from JP3060 successfully methylated myricetin at the 3′ position (Figure 6E), consistent with the hypothesis that the accumulation of low *MOMT4* mRNA plays a role in the mutant phenotype (Figure 7).

Transgenic Plant Experiments Support the Hypothesis That Sl-MOMT4 Is a Myricetin 3′ *O*-Methyltransferase

Two reverse genetic approaches were used to test the hypothesis that mutation of the *MOMT4* gene caused the increased monomethylation phenotype. First, transgenic mutant plants were obtained in which *MOMT4* was expressed in the *momt4* JP3060 mutant using the *AT2* promoter, which previously was shown to confer specific expression of GFP-GUS reporter in the type 1 trichomes (Schilmiller et al., 2012a) (see Methods for the details). Three of the four T1 transgenic complementation lines (C-7, -8, and -9 in Supplemental Figure 7) exhibited reversal of JP3060 mutant phenotype by LC-ToF-MS in negative mode. In addition to complementation testing, RNA interference (RNAi) experiments were performed to test the hypothesis that lower gene expression of MOMT4 in the M82 background by RNAi would shift the composition of methylated myricetins toward monomethylated myricetin (see Methods for the details). Three of the four T1 transgenic lines tested (R-6, -7, and -8 in Supplemental Figure 7) exhibited lower dimethylated and trimethylated myricetin and also lower ratios of 2Me-M/1Me-M compared with that of M82. Taken together, these transformation experiments support the hypothesis that MOMT4 from M82 tomato has myricetin 3′ *O*-methyltransferase activity in vivo.

The Heinz 1706 *S. lycopersicum* Cultivar Is Defective in *MOMT4*

The lack of recognizable *MOMT4* sequence in the Heinz 1706 reference genome could be due to an assembly error or absence of this gene from this cultivar (Da Silva et al., 2013; Hirsch et al., 2014). Consistent with the absence of a functional *MOMT4* gene, extracts from Heinz 1706 trichomes contain 3-methyl myricetin, but lack the 3,3′-methylated product (Figure 3; Supplemental Figure 8). To discover the lesion that led to this phenotype, we sought to identify and sequence the Heinz *MOMT4* allele, but could not amplify this sequence using different PCR primers that give positive results with M82 DNA (Figure 8). The inability to identify *MOMT4* sequences in the Heinz 1706 genome assembly or by PCR of genomic DNA and associated accumulation of 3-methyl myricetin strongly suggested that this variety is a *momt4* mutant.

To test whether Heinz 1706 is unique in this regard, trichome metabolites were analyzed for two other *S. lycopersicum* cultivars (Supplemental Figure 8). Negative mode LC-ToF-MS revealed that variety Ailsa Craig resembles Heinz 1706, where only monomethylated myricetin is detected. In contrast, variety Castlemart accumulates mono-, di-, and trimethylated myricetins in relative amounts similar to those seen in M82. These results indicate that differences in myricetin methylation patterns are found in other cultivated tomato varieties.

```
M82     201 ETIDVGGGLGISLASIISKYPNIKGINFDLPHVIKDAPTYEGIEHVGGDM 250
JP446   201 ETIDVGGGLGISLASIISKYPNIKGINFDIPHVIKDAPTYEGIEHVGGDM 250
JP3060  201 ETIDVGGGLGISLASIISKYPNIKGINFDLPHVIKDAPTYEGIEHVGGDM 250

                                    ...

M82     301 YPETNLLSKHLFALDISMMIMFHGGKERTKQQFEDLAKQAGFTSIKVMAR 350
JP446   301 YPETNLLSKHLFALDISMMIMFHGGKERTKQQFEDLAKQAGFTSIKVMAR 350
JP3060  301 YPETNLLSKHLFALDISMMIMFNGGKERTKQQFEDLAKQAGFTSIKVMAR 350
```

Figure 9. JP446 and JP3060 Mutants Have Point Mutations in the Protein Coding Sequence of MOMT4.

The differences in the protein sequences are highlighted with black shading. Protein motifs conserved among previously known plant *O*-methyltransferases are underlined (Lam et al., 2007).

DISCUSSION

Combining Classical Mutagenesis with Metabolic Profiling in the *Solanum* Genus Is an Efficient Way to Discover Unannotated Genes of Specialized Metabolism

Efficient and inexpensive sequencing technologies and mass spectrometry methods continue to transform the discovery of specialized metabolic pathway enzymes (Schilmiller et al., 2012a) in both model and nonmodel organisms (Rounsley and Last, 2010; Winzer et al., 2012). While these approaches will continue to increase the speed and breadth of study of metabolic pathways, they rely on the ability to find candidate sequences in EST libraries and genome assemblies and infer enzymatic activities of novel enzymes from primary sequence. In contrast, forward genetic screens only rely on the ability to detect differences in phenotype associated with induced or natural genetic variation (for example, Goulet et al., 2012; Schilmiller et al., 2012b). The combination of in vitro biochemistry and mutant analysis is especially powerful because it can corroborate the in vivo importance of an enzymatic activity.

A forward genetic screen for mutations that influence *S. lycopersicum* metabolite profiles uncovered three independent M2 mutants that accumulate monomethylated myricetin (Figure 2; Supplemental Table 2). Analysis of the JP117 mutant by positive ion mode LC-MS/MS led to the identification of the monomethylated species as 3-methyl myricetin, lacking methylation at the 3′ position (Figures 1 and 3; Supplemental Figure 1). Genetic mapping of the mutation revealed that the responsible gene is on the bottom of chromosome 6 (Supplemental Figure 5), which created a quandary because no intact candidate flavonoid 3′ *O*-methyltransferase gene was found in this region of the *S. lycopersicum* Heinz 1706 variety reference genome sequence (Tomato Genome Consortium, 2012). A combination of genetic analysis, comparison of the reference genome to assemblies of genomic DNA of related wild tomato species, and mutant cDNA and genomic DNA sequencing led to the identification of a previously unannotated flavonoid *O*-methyltransferase, Sl-*MOMT4*, as the *S. lycopersicum* M82 gene affected in the mutants. The wild-type enzyme was shown to have myricetin 3′ *O*-methyltransferase activity in vitro, and MOMT4 protein from JP446 had lost enzymatic activity (Figure 6), while mutants JP117 and JP3060 have reduced accumulation of *MOMT4* mRNA in trichomes (Figure 7). Transformation experiments provided further support for the role of *MOMT4* in myricetin methylation: transgenic expression of 35S promoter-*MOMT4*-RNAi *S. lycopersicum* M82 transgenics caused an increase in monomethylated myricetin and *MOMT4* cDNA expression using a Type 1 glandular secreting trichome promoter (Schilmiller et al., 2012b) complemented the JP3060 mutation (Supplemental Figure 7).

The *S. lycopersicum momt4* Mutations Are Not Typical of EMS Mutagenesis

DNA sequence analysis of the three *momt4* mutants yielded results that differ from the expected G:C to A:T transition mutations. The textbook view is that EMS causes guanine ethylation, which leads to replacement of the complementary cytosine with thymine following the first round of DNA replication. This is followed by replacement of the O^6-ethylguanine by adenine in the next round of DNA replication, leading to the change of the original G:C base pair to an A:T mutant base pair in the final mutation. In contrast, both JP446 and JP3060 have noncanonical G:C to T:A changes. Unexpected types of EMS mutations are surprisingly common in *S. lycopersicum* mutants, including the M82 collection we screened, with nucleotide deletions and nonstandard base pair changes reported in a variety of genes (Barry et al., 2012; Jones et al., 2012; Yifhar et al., 2012). These observations suggest that DNA damage repair in cultivated tomato is unusual and worthy of study. The third high 3-methyl myricetin mutant analyzed, JP117, also does not have a canonical EMS point mutation. Because it was not possible to amplify the JP117 *momt4* allele, we cannot evaluate the precise change in nucleotide sequence. Thus, we cannot rule out the possibility that this line is a seed contaminant of Heinz 1706 or another wild-type cultivar that accumulates 3-*O*-methylmyrecitin (for example, Ailsa Craig; Supplemental Figure 8). This question should resolve as genome sequence for other tomato cultivars become available.

Sl-*MOMT4* Is an Example of an Emerging Theme: Presence/Absence Polymorphisms for *Solanum* Trichome Specialized Metabolism Genes within and across Species

Genome resequencing of individuals from the same species recently led to the identification of increasing numbers of examples of genome differentiation leading to phenotypic diversity in a species. These studies are especially powerful when comparing sequences from an individual of interest with those of the reference genome in the same species. Resequencing of individuals and comparative analysis with the reference genome in the same species was conducted in various plant genomes, including *Arabidopsis* (Jander et al., 2002; Ossowski et al., 2008; Weigel and Mott, 2009; Cao et al., 2011; Schneeberger et al., 2011) and maize (Springer et al., 2009; Swanson-Wagner et al., 2010; Hirsch et al., 2014). These studies revealed single nucleotide polymorphisms, small insertions and deletions, as well as copy number variations and larger presence/absence variations within the species. These and other studies led to the concepts of core genome (sequences that commonly exist in all individuals), dispensable genome (sequences that exist only in a subset of individuals), and pangenome (the combination of core and dispensable genomes) to describe the evolution of plant genomes (Morgante et al., 2007; Flowers and Purugganan, 2008). This genome differentiation contributes to phenotypic diversity. For instance, recent studies on the grape (*Vitis vinifera*) cultivar Tannat revealed polyphenol biosynthesis genes specific to this individual and not present in the reference genome. This work revealed that gene family expansion in cultivar Tannat led to high polyphenol accumulation phenotypes in this individual (Da Silva et al., 2013). These and other studies reinforce the notion that a reference genome cannot always be relied on for discovery of genes that contribute to interesting phenotypic variation, especially for fast-evolving genes that potentially contribute to plant adaptation under different environments.

Divergence in sequence and function of genes and enzymes, as well as in presence versus absence of genes, is also found in secreting glandular trichome specialized metabolism of cultivated

tomato and related *Solanum* species. Terpenes provide the best-established examples thus far, with type 6 glands producing diverse mono- or sesquiterpenes through cisoid diprenylphosphate intermediates in *S. lycopersicum* and *S. habrochaites* (Sallaud et al., 2009; Schilmiller et al., 2009; Gonzales-Vigil et al., 2012; Matsuba et al., 2013). Strong phenotypic diversity is also seen in acylsugars produced in type 1 glands of various *S. habrochaites* accessions (Kim et al., 2012; Ghosh et al., 2013). It was recently demonstrated that allelic variation at the *AT2* gene in this species is responsible for differences in acylsucrose R2 acetylation in *S. habrochaites* populations across its geographical range (Kim et al., 2012). Genetic variation in the trichome-expressed *CPS2* diterpene synthase gene is also associated with labdanoid diterpene accumulation in tobacco (*Nicotiana tabacum*) trichomes (Sallaud et al., 2012).

Work on *Solanum* trichome flavonoid *O*-methyltransferases illustrates both the value and limitations of comparative biochemistry when only a single high quality reference sequence is available. Our results indicated that, in contrast to *S. habrochaites* LA1777, the Sl-*MOMT1* gene is defective in both the reference sequence Heinz 1706 and in M82 (Schmidt et al., 2011; this study). The results described above indicate that *MOMT4* provides 3′-*O*-methylation activity in M82 cultivated tomato and presumably in the wild tomatoes *S. pimpinellifolium* and *S. pennellii* (Figure 4) but not in *S. lycopersicum* Heinz 1706. F2 mapping of the *momt4* JP117 mutation, and analysis of the *S. pennellii* LA0716 × *S. lycopersicum* M82 IL6-4 showed that the Sl-*MOMT4* and Sp-*MOMT4* are genetically linked to the Sl-*MOMT1* gene at the bottom of chromosome 6 (between nucleotides 44,524,611 and 46,041,039; Supplemental Figures 2 and 5). However, our PCR and DNA sequencing analysis of the defective Sl-*MOMT1* region shows that in M82, as in Heinz, *MOMT1* is flanked by *MOMT3* (not annotated in the Heinz 1706 reference genome) upstream of it and by a WD-40 repeat protein gene (Solyc06g083460) downstream from it. Thus, while the two genes may be near each other, *MOMT4* is not directly adjacent to *MOMT1*, which is at position 45,144,339 to 45,145,525 (Supplemental Figure 2).

Sl-MOMT1 and MOMT4 Have Diverged Biochemically

This investigation shows that, in *S. lycopersicum* M82, the *MOMT4* gene encodes 3′ *O*-methylation activity on myricetins in the trichomes. Incubation of Sl-MOMT4 with myricetin yielded 3′-methyl myricetin and only trace amounts of 3′,5′-dimethyl myricetin (Figure 6; Supplemental Figure 4), consistent with the observation that M82 tomato trichomes do not contain myricetins methylated at the 5′ position (Figure 3). In contrast, Sh-MOMT1 added a methyl group to the 5′ position of 3′-methylmyricetin, as well as the initial methyl group to the 3′ position as previously described by Schmidt et al. (2011). While the Sp-MOMT1 enzyme has not been directly tested for activity, the observation that the IL6-3 and IL6-4 lines, which have the Sp-*MOMT1* gene, possess myricetins methylated at both 3′ and 5′ position suggests that Sp-MOMT1 is also a 3′/5′ MOMT enzyme (Supplemental Table 1). Thus, the reason for the lack of myricetins methylated at the 5′ position in M82 tomato appears to be due to lack of a functional *MOMT1* gene. Based upon analysis of the available sequences for various *Solanum* species, we conclude that *S. pennellii* has both *MOMT4* and *MOMT1* genes.

Incomplete DNA sequences prevent conclusive evaluation of other tomato species. For example, the available *S. pimpinellifolium* genome sequence contains only a partial *MOMT1* sequence and existing genomic DNA sequence resources prevents conclusive evaluation of whether *S. habrochaites* also contains the *MOMT4* gene. Furthermore, different accessions of the cultivated tomato are polymorphic for Sl-*MOMT4*, with M82 having a functional gene and Heinz 1706 lacking a functional copy of the gene, which might even be completely deleted in that accession (Figure 8). This intraspecific difference leads to alterations in chemical composition of modified myricetins in the two accessions, with M82 accumulating multiply methylated myricetin and Heinz 1706 plants containing mono-methylated myricetin (Figure 3). Our results further suggest a model where *MOMT4* and *MOMT1* are the results of gene duplication that occurred prior to the split between *S. lycopersicum* and *S. pennellii*, followed by more recent losses of functional *MOMT1* and *MOMT4* genes during breeding of cultivated tomato. This work provides another example of the strong plasticity of specialized metabolism in trichomes of cultivated tomato and its wild relative.

METHODS

Plant Growth Conditions

Solanum lycopersicum M82 cultivated tomato seeds were obtained from the Tomato Genetic Resource Center (http://tgrc.ucdavis.edu/). Tomato EMS M2 family mutants (Menda et al. 2004) were kindly supplied by Dani Zamir (Hebrew University, Rehovot, Israel). Mutants identified from this study were donated to the Tomato Genetic Resource Center when seeds were available and the accession IDs are listed in Supplemental Table 2. Thirty-two plants were germinated on filter papers, transplanted to small pots, and grown in each flat including two M82 wild-type plants. Plants were randomly located within the flat and grown for 3 weeks under the growth conditions previously described (Schilmiller et al., 2010a).

Phenotypic Validation and Structural Analysis of Methylated Myricetins Using Positive Mode LC-MS/MS Method

Comparative analysis of methylated myricetins in the various genotypes was performed using leaf dip extracts from M82 wild type, JP117 mutant, Heinz 1706, and ILs 6-3 and 6-4 plants grown for 3 weeks under the growth chamber conditions described above. The extracts were analyzed according to methods described (Li et al., 2013) with some modifications. In brief, HPLC separation of myricetins was achieved using a Thermo β-Basic C18 column (100 mm × 1.0 mm, 3 μm) at 50°C with solvent A 0.15% formic acid in water and solvent B acetonitrile. The Q-TRAP 3200 mass spectrometer was operated in positive ion mode for all analyses. For determining positions of methyl groups in the methyl-myricetins, enhanced product ion scanning was used to generate MS/MS spectra. For relative quantification of methyl myricetins, a selected ion monitoring method was used for m/z 333 (1Me-M), 347 (2Me-M), 361 (3Me-M), 375 (4Me-M), and 181 (propyl-4-hydroxybenzoate internal standard).

Generation of Genetic Cross Progeny and Genetic Mapping for Mutant JP117

JP117 was backcrossed to M82 wild type in a reciprocal manner, resulting in M82 × JP117 and JP117 × M82 plants. Backcross F1 and self-cross F2 progeny plants were used for phenotypic studies.

JP117 mutant was outcrossed to LA0716 *Solanum pennellii* and F2 progeny plants were generated as a mapping population. Mapping was performed with publicly available codominant amplified polymorphic

sequence (CAPS) markers from the Sol Genomics Network (http://solgenomics.net/, markers 1-4 and 13 from Supplemental Figure 5). When not available, CAPS markers were generated in this study (markers 5 to 12 from Supplemental Figure 5). The polymorphic sequences between *S. lycopersicum* and *S. pennellii* were identified based on genomic sequence and trichome ESTs for the two species (http://solgenomics.net/, SL2.31 chromosome sequences; Schilmiller et al., 2010b). CAPS markers were generated using the CAPS designer program (http://solgenomics.net/tools/caps_designer/caps_input.pl/). Primer sequences and the types of restriction enzymes for individual markers are listed in Supplemental Table 3.

Genotyping was performed by genomic DNA PCR with RedTaq mix (Sigma-Aldrich), followed by digestion with restriction enzymes (New England Biolabs). The PCR thermocycle conditions were as follows: 40 times for 45 s at 94°C, 45 s at 55°C, and 1 min at 72°C. This thermocycle protocol was used for other PCR experiments in the rest of this study unless otherwise specified. The PCR products were incubated with restriction enzymes for 4 h at 37°C.

BLAST Analysis to Identify MOMT Homologs

BLAST analysis was performed to identify MOMT homologs in *S. lycopersicum* (http://solgenomics.net/, SL2.31 chromosome sequence) using previously characterized *Solanum habrochaites MOMT1* and *MOMT2* gene sequences (Schmidt et al., 2011). To identify MOMT homologs in wild species of tomato, genome shotgun sequences of *S. pennellii* (kindly provided by Alisdair Fernie and Bjoern Usadel, Max Planck Institute of Molecular Plant Physiology, Potsdam-Golm, Germany), *S. pimpinellifolium* (http://solgenomics.net/tools/blast/index.pl), and trichome EST libraries (http://bioinfo.bch.msu.edu/trichome_est; Schilmiller et al., 2010b) were used.

Testing Chromosomal Locations of Sl-*MOMT* Homologs

The chromosomal location of five Sl-*MOMT* genes identified from BLAST analysis (Sl-*MOMT1*, 3, 2a, and 2b) was validated by mapping them on *S. pennellii* ILs (Eshed and Zamir, 1995). The validation was performed by identifying a polymorphic sequence for each gene and looking for the presence of the *S. pennellii* LA0716 polymorphism on the four *S. pennellii* ILs covering chromosome 6. In each case, the *S. pennellii* polymorphism was found associated with the expected IL. The generation of CAPS markers and genotyping was performed as described above. See Supplemental Table 4 for primer sequences and the list of restriction enzymes.

MOMT4 Sequence Analysis

Sl-*MOMT4* from *S. lycopersicum* M82 (GenBank accession KF740343) and Sl-*MOMT4* from IL6-4 were amplified using genomic DNA with primers SlMOMT3-P1 and SlMOMT4-P6 (*S. lycopersicum* M82 wild type) and SlMOMT3-P1 to IL6-4MOMT4-cloningP4 (IL6-4) (Supplemental Table 5). The fragments were ligated into pGEMT-easy vector (Promega) and sequenced. Sp-*MOMT4* gene is obtained from the database (http://trichome.msu.edu/). MOMT4 coding sequences from JP446 and JP3060 mutants were PCR amplified from cDNA and the products were sequenced as described for M82 above.

PCR reactions with primers SlMOMT4-P1 to SlMOMT4-P6 were performed with KOD polymerase (Novagen) using genomic DNA obtained from either *S. lycopersicum* M82, Heinz 1706, or JP117 mutant plant leaves. For amplification of Sl-*MOMT3*, SlMOMT3-P1 and SlMOMT3-P2 primers were used (Supplemental Table 5). The PCR thermocycle conditions were as follows: 35 cycles for 30 s at 94°C, 30 s at 55°C, and 3 min at 70°C. PCR products were separated by agarose gel, stained with ethidium bromide, and photographed under UV light.

Phylogenetic Analysis

The phylogenetic tree (Figure 4) was generated by sequence alignment (alignment parameters were protein sequence, pairwise alignment, gap opening penalty:10, gap extension penalty: 0.1, multiple alignment, gap opening penalty: 10, gap extension penalty: 0.2, protein weight matrix: Gonnet residue-specific penalties: ON, hydrophilic penalties: ON, gap separation, distance: 4, end gap separation: OFF, use negative matrix: OFF, delay divergent cutoff [%]: 30.) (Supplemental Data Set 1) using ClustalW (Thompson et al., 1994), and tree construction with statistical tests (parameters for phylogeny reconstruction were neighbor-joining method [Saitou and Nei, 1987], bootstrap [Felsenstein, 1985], n = 1000, amino acid, Poisson model, rate among sites: uniform rates gaps/missing, data treatment: complete deletion, traditional tree without modification for graphics) using MEGA6 (Tamura et al., 2011).

Analysis of *MOMT4* Gene Expression in Trichomes

Total RNA was isolated from M82 intact stems and petioles, isolated total stem and petiole trichomes, and stems and petioles with trichomes removed using a Qiagen RNeasy kit (Qiagen). Trichomes were harvested by freezing tissues in liquid nitrogen and scraping off the frozen tissues. Reverse transcription was performed with 1 μL of total RNA using SuperScriptII reverse transcriptase (Invitrogen), followed by PCR with RedTaq mix (Sigma-Aldrich) and primers SlMOMT4-P1 and SlMOMT4-P6 (Supplemental Table 5). EF1a was used as a control, and this assay employed primers EF1a F1 and EF1a R1 (Supplemental Table 5). PCR products were sequenced to confirm the amplification of MOMT4.

Quantitative PCR was performed to quantify the accumulation of *MOMT4* mRNA in M82 wild-type and mutant plants. Total RNA was isolated from isolated total stem and petiole trichomes of M82 and mutants including JP117, JP446, and JP3060, and cDNA was obtained as described above. MOMT4 cDNA was amplified with primers SlMOMT4-F3 and SlMOMT-R3, and EF1a control with EF1a F2 and R2 (Supplemental Table 5). Quantitative PCR was performed using SYBR green master mix (Applied Biosystems) following the manufacturer's protocols. Standard curves were made for EF1a control and MOMT4 with 10-fold dilutions of cDNA concentrations ranging from 0.001 to 10 μM. The signal for MOMT4 was normalized to EF1a control. cDNA (20 ng/μL) was used for EF1a, whereas 200 ng/μL cDNA was used for MOMT4 due to lower expression of MOMT4.

Chemical Screening of Tomato EMS M2 Family Mutants and Statistical Analysis of M2 Mutant Metabolite Phenotypes

A cultivated tomato (*S. lycopersicum*, cultivar M82) EMS mutant population of M2 mutant families (Menda et al., 2004; Supplemental Figure 9) was screened for changes in trichome metabolites by LC-ToF-MS. Fifty-eight M2 families were randomly chosen from the tomato EMS mutant population, and the chemical profiles of 1387 M2 plants were analyzed and compared with those of control M82 wild-type plants grown in the same flats and growth chamber. The single leaf dip extraction method and a 5-min negative ion mode LC-ToF-MS analysis were performed for mutant screening as described (Schilmiller et al., 2010a). Surface metabolites were extracted for 60 s with gentle rocking and dry weights of the extracted leaf samples were measured following drying at 50°C. Peak areas were integrated for the individual 33 analytical signals detected (Supplemental Table 6) using QuanLynx software (Waters) and normalized to internal standard (propyl-4-hydroxybenzoate; Sigma-Aldrich) and leaf dry weight. The LC-ToF-MS chemical analysis generated a list of thousands of analytical signals, defined as having a unique combination of liquid chromatography retention time and mass-to-charge ratio (m/z) in the ToF-MS (Schilmiller et al., 2010a). The identified analytical

signals were evaluated using parallel targeted and nontargeted data analyses (Supplemental Figure 10). Thirty-three analytical signals were selected for targeted data analysis (Supplemental Table 6), based on a previous study that identified relatively abundant trichome metabolites (Schilmiller et al., 2010a). Although nontargeted analysis was performed to complement the possibility that targeted analysis might fail to identify novel mutant phenotypes, nontargeted analysis did not provide additional discovery to targeted analysis in this study. A total of 1387 M2 mutants from 58 families were screened, obtaining 223 (16%) putative mutants. These were self-pollinated, with 175 producing M3 seed for rescreening. In total, 24 of the M2 lines had consistent phenotypes in the M3 progeny (Supplemental Table 7). The 24 identified mutants revealed altered chemistry in different classes of metabolites including methylated and glycosylated flavonoids, the glycoalkaloid tomatine, and acylsugars (Supplemental Table 2). Multiple independent mutants were found for each of five types of trichome chemistry: methylated myricetins, a myricetin glycoside, increased kaempferol 3-*O*-rutinoside, acylsugar S4:15, and an unannotated analytical signal with *m/z* 493.3.

The normalized data set was used for targeted and nontargeted data analyses. First, median and median absolute deviation were calculated as described (Ambrósio et al., 2008) to identify outliers altered in the 35 analytical signals. All comparisons were made to plants grown in the same flat of 32 plants to control for environmentally influenced flat differences. When the outliers met both of two cutoffs, median ± 5 median absolute deviation and >3-fold change compared with the median, they were considered M2 putative mutants. In nontargeted analysis, principal component analysis (PCA) was applied to identify putative mutants that targeted analysis might have failed to discover. PCA was performed using Markerlynx software (Waters) with the same data set used for targeted analysis.

Once M2 putative mutants were identified, seeds were collected from the self-pollinated M3 progeny of the individual M2 putative mutants. Identical growth conditions, including temperature and light conditions, and chemical assay methods were applied to M3 progeny testing as to M2 mutant screening. Each flat contained 32 plants, consisting of four M82 wild-type plants and seven different types of mutants with four replicates, and all analyses were performed for each flat considering potential environmental variations between flats. Targeted and nontargeted analyses were performed to test chemical phenotypes in M3 progeny. In targeted analysis, two cutoffs were used to identify mutants from M82 wild type plants: (1) >3-fold change in the mean between mutant and M82 wild type; (2) statistically significant alteration corresponding to $P < 0.05$ from Student's *t* test. In addition to PCA, the partial least squares discriminant analysis supervised method was also employed for nontargeted data analysis in M3 progeny. Partial least squares discriminant analysis allows identification of minor factors contributing to the separation between mutant and wild-type plants and searching for the correlation among these analytical signals.

Allelism Tests

JP117 and JP446 mutants were crossed in a reciprocal manner, resulting in a single JP117 (female) × JP446 (male) cross plant and three from independent JP446 × JP117 plants. Progeny from the crossed plants were grown for 3 weeks under growth chamber conditions as described above. Their chemical phenotypes were analyzed by single leaf dip extraction and negative LC-ToF-MS analysis.

The cross plants were genotyped to confirm that they were not the result of self-crossing by genomic DNA PCR with primers SlMOMT3-P1 and SlMOMT-R4 (Supplemental Table 5) followed by sequence analysis. Genomic DNA was isolated from all six progeny plants from a JP117 × JP446 cross plant and two randomly chosen progeny from each of three independent JP446 × JP117 cross plants.

Recombinant MOMT4 Enzyme Assay

The full-length open reading frame of *MOMT4* was cloned using cDNA from M82 wild type and mutants JP446 and JP3060. PCR was performed with primers SlMOMT4-F4 and SlMOMT4-R2 (Supplemental Table 5) and proofreading *Pfu* DNA polymerase (Agilent). The thermocycling conditions were: 30 times each for 45 s at 94°C, 45 s at 55°C, and 1.5 min at 72°C. The PCR products were digested with restriction enzymes *Hind*III and *Xho*I (NEB) and ligated into pET28b vector (Novagen). The construct was transformed into BL21 Rosetta (Novagen). An *Escherichia coli* colony containing the correct construct was grown in Luria-Bertani medium at 37°C to an optical density at 600 nm of 0.8 at which time cultures were induced with 0.05 mM isopropyl-β-D-thiogalactopyranoside and incubated at 16°C for 48 h with aeration by shaking. The induced cultures were lysed by sonication in lysis buffer (50 mM Tris, 10 mM NaCl, 1 mM EDTA, 10% glycerol, and 14 mM β-mercaptoethanol, pH 8.0) as described (Schmidt et al., 2011). The recombinant protein was purified using nickel-affinity chromatography including washing step with 20 mM imidazole followed by an elution step with 200 mM imidazole. Enzyme assays were performed following the methods described (Schmidt et al., 2011). Approximately 5 μg of the purified recombinant protein was assayed in 500 μL of the lysis buffer containing 250 μM myricetin (Sigma-Aldrich) and 200 μM *S*-adenosylmethionine (Perkin-Elmer Instruments) substrates. After 30 min of incubation at room temperature, the reaction was terminated by adding 50 μL of 6 N HCl. A total of 500 μL of ethyl acetate was added to the reaction to extract the assay product. After centrifugation for 3 min, the upper phase was removed and evaporated to dryness. The residue was dissolved in 50 μL 50% ethanol and used for product analysis with negative mode LC-ToF-MS (Schilmiller et al., 2010a) and positive mode LC-MS/MS (Schmidt et al., 2011; Li et al., 2013). Thin-layer chromatography analysis with ^{14}C-SAM was performed using the same conditions described (Schmidt et al., 2011), namely, 200 μM flavonol substrate and 1.7 μM ^{14}C-SAM. Under these conditions, the flavonol substrate was saturating and the reaction increased linearly with doubled ^{14}C-SAM substrate.

Generation of Transgenic Plants and Phenotypic Analyses

Agrobacterium tumefaciens-mediated transformation of cotyledon explants was performed using a published method (McCormick, 1991). In both cases, four T1 plants from each of three independent T0 lines were phenotypically analyzed using the single leaf dip metabolite extraction and negative ion mode LC-ToF-MS analysis as described above. For transgenic complementation testing, we modified the pK7WG2 vector so that it contains the type 1 gland trichome-specific Sl-*AT2* promoter (Schilmiller et al., 2012b) instead of the 35S promoter. The 35S promoter was removed from the pK7WG2 vector by restriction enzyme digestion and replaced with a fragment carrying the *AT2* promoter (see Supplemental Figure 11 for details). The full-length cDNA sequence of MOMT4 from M82 was amplified using the primers SlMOMT4-CF and SlMOMT4-CR (Supplemental Table 5). The resulting product was cloned into pENTR/D-TOPO, then moved into the modified pK7WG2 vector, and the construct was transformed into JP3060 mutants. To generate RNAi lines, a MOMT4-specific fragment of 442 bp, located in the 5′-region of *MOMT4*, was amplified by PCR with the gene-specific primers SlMOMT4-RNAiF and SlMOMT4-RNAiR. The purified PCR product was introduced in the Gateway system entry vector (pENTR/D-TOPO) and then transferred as an inverted repeat under the control of the 35S promoter in the RNAi destination vector pHELLSGATE12 (Helliwell and Waterhouse, 2003) for transformation into M82 wild-type plants.

Accession Numbers

Sequence data from this article can be found in the GenBank/EMBL data libraries under accession number KF740343.

Supplemental Data

The following materials are available in the online version of this article.

Supplemental Figure 1. Enhanced Product Ion MS/MS Spectra for [M+H]+ Ions of Methylated Myricetins.

Supplemental Figure 2. Schematic Representation of Candidate *O*-Methyltransferases and WD-40 Repeat Gene on Chromosome 6.

Supplemental Figure 3. Alignment of Genomic DNA Sequences of *MOMT4* from *S. lycopersicum*, *S. pennellii*, and IL6-4.

Supplemental Figure 4. Enhanced Product Ion MS/MS Analysis Identified Monomethylated Myricetin Product from in Vitro Enzyme Assay as 3′-Methylmyricetin.

Supplemental Figure 5. The JP117 Mutation Maps to the Bottom of Chromosome 6.

Supplemental Figure 6. Phenotypic Results from Reciprocal Crosses between Mutants JP446 and JP117 Demonstrate That These Mutations Fail to Complement.

Supplemental Figure 7. Methylated Myricetin Profiles in Sl-MOMT4 Transgenic Plants.

Supplemental Figure 8. Methylated Myricetin Profiles in *S. lycopersicum* Varieties.

Supplemental Figure 9. Structure of the Mutant Population and Workflow of This Study.

Supplemental Figure 10. EMS Mutant Screening Workflow.

Supplemental Figure 11. Schematic View for the Generation of Sl-*AT2* Promoter Fused pK7WG2 Vector.

Supplemental Table 1. The Distribution of Myricetin Derivative Structures and MOMT Genes in *Solanum* Plants.

Supplemental Table 2. Chemical Phenotypes of the 24 Mutants Identified from This Screening.

Supplemental Table 3. The List of Codominant Amplified Polymorphic Sequence Markers Generated to Map JP117 Mutation.

Supplemental Table 4. The Codominant Amplified Polymorphic Sequence Marker Primers and Products Generated to Map the Location of MOMTs on Chromosome 6.

Supplemental Table 5. The Primers Used for Identification and Characterization of Sl-*MOMT4.*

Supplemental Table 6. The List of 33 Analytical Signals Used for Targeted Data Analysis.

Supplemental Table 7. Summary of Mutant Screen Results.

Supplemental Data Set 1. Clustal Sequence Alignment for OMTs Listed in Figure 4.

ACKNOWLEDGMENTS

Funding was from National Science Foundation Grants DBI-0604336 and IOS-1025636, U.S. Department of Energy Grant DE-FG02-91ER20021 (for support of J.K.), and Michigan AgBioResearch Project MICL02143 (A.D.J.). We thank Dani Zamir (Hebrew University of Jerusalem, Rehovot, Israel) for providing seeds of the EMS mutant lines and Kathleen Imre for generating transgenic lines. We also thank other members of the *Solanum* Trichome Project for discussions and ideas and Ramin Vismeh of the MSU Mass Spectrometry and Metabolomics Core for analysis of MOMT4 enzyme assay products. We thank Alisdair Fernie and Bjoern Usadel (Max Planck Institute of Molecular Plant Physiology, Golm, Germany) for providing *S. pennellii* genome sequence. IL6-3 and IL6-4 seeds were obtained from the C. M. Rick Tomato Genetics Resource Center (University of California, Davis, CA).

AUTHOR CONTRIBUTIONS

J.K., E.P., Y.M., and R.L.L. designed the research. J.K., Y.M., J.N., D.H., and A.L.S. performed the research. J.K., Y.M., J.N., A.L.S., and A.D.J. analyzed data. J.K., E.P., and R.L.L. wrote the article.

Received July 3, 2014; revised July 25, 2014; accepted July 31, 2014; published August 15, 2014.

REFERENCES

Ambrósio, S.R., Oki, Y., Heleno, V.C., Chaves, J.S., Nascimento, P.G., Lichston, J.E., Constantino, M.G., Varanda, E.M., and Da Costa, F.B. (2008). Constituents of glandular trichomes of *Tithonia diversifolia*: relationships to herbivory and antifeedant activity. Phytochemistry **69:** 2052–2060.

Barry, C.S., Aldridge, G.M., Herzog, G., Ma, Q., McQuinn, R.P., Hirschberg, J., and Giovannoni, J.J. (2012). Altered chloroplast development and delayed fruit ripening caused by mutations in a zinc metalloprotease at the *lutescent2* locus of tomato. Plant Physiol. **159:** 1086–1098.

Bolger, A., et al. (2014). The genome of the stress-tolerant wild tomato species *Solanum pennellii.* Nat. Genet. http://dx.doi.org/.

Braca, A., Bilia, A.R., Mendez, J., and Morelli, I. (2001). Myricetin glycosides from *Licania densiflora.* Fitoterapia **72:** 182–185.

Buer, C.S., Imin, N., and Djordjevic, M.A. (2010). Flavonoids: new roles for old molecules. J. Integr. Plant Biol. **52:** 98–111.

Cao, J., et al. (2011). Whole-genome sequencing of multiple *Arabidopsis thaliana* populations. Nat. Genet. **43:** 956–963.

Chae, L., Kim, T., Nilo-Poyanco, R., and Rhee, S.Y. (2014). Genomic signatures of specialized metabolism in plants. Science **344:** 510–513.

Da Silva, C., et al. (2013). The high polyphenol content of grapevine cultivar tannat berries is conferred primarily by genes that are not shared with the reference genome. Plant Cell **25:** 4777–4788.

Eshed, Y., and Zamir, D. (1994). A genomic library of *Lycopersicon pennellii* in *Lycopersicon esculentum* - A tool for fine mapping of genes. Euphytica **79:** 175–179.

Eshed, Y., and Zamir, D. (1995). An introgression line population of *Lycopersicon pennellii* in the cultivated tomato enables the identification and fine mapping of yield-associated QTL. Genetics **141:** 1147–1162.

Falara, V., Akhtar, T., Nguyen, T.T., Spyropoulou, E.A., Bleeker, P.M., Schauvinhold, I., Matsuba, Y., Bonini, M.E., Schilmiller, A.L., Last, R.L., Schuurink, R.C., and Pichersky, E. (2011). The tomato (*Solanum lycopersicum*) terpene synthase gene family. Plant Physiol. **157:** 770–789.

Felsenstein, J. (1985). Confidence limits on phylogenies: An approach using the bootstrap. Evolution **39:** 783–791.

Flowers, J.M., and Purugganan, M.D. (2008). The evolution of plant genomes: scaling up from a population perspective. Curr. Opin. Genet. Dev. **18:** 565–570.

Furr, M., and Mahlberg, P.G. (1980). Histochemical analyses of laticifers and glandular trichomes in *Cannabis sativa.* J. Nat. Prod. **44:** 153–159.

Gang, D.R. (2005). Evolution of flavors and scents. Annu. Rev. Plant Biol. **56:** 301–325.

Ghosh, B., Westbrook, T.C., and Jones, A.D. (2013). Comparative structural profiling of trichome specialized metabolites in tomato (*Solanum lycopersicum*) and *S. habrochaites*: acylsugar profiles revealed by UHPLC/MS and NMR. Metabolomics **406:** 171–182.

Glas, J.J., Schimmel, B.C., Alba, J.M., Escobar-Bravo, R., Schuurink, R.C., and Kant, M.R. (2012). Plant glandular trichomes as targets for breeding or engineering of resistance to herbivores. Int. J. Mol. Sci. **13:** 17077–17103.

Gonzales-Vigil, E., Hufnagel, D.E., Kim, J., Last, R.L., and Barry, C.S. (2012). Evolution of TPS20-related terpene synthases influences chemical diversity in the glandular trichomes of the wild tomato relative *Solanum habrochaites.* Plant J. **71:** 921–935.

Goulet, C., Mageroy, M.H., Lam, N.B., Floystad, A., Tieman, D.M., and Klee, H.J. (2012). Role of an esterase in flavor volatile variation within the tomato clade. Proc. Natl. Acad. Sci. USA **109:** 19009–19014.

Heim, K.E., Tagliaferro, A.R., and Bobilya, D.J. (2002). Flavonoid antioxidants: chemistry, metabolism and structure-activity relationships. J. Nutr. Biochem. **13:** 572–584.

Helliwell, C., and Waterhouse, P. (2003). Constructs and methods for high-throughput gene silencing in plants. Methods **30:** 289–295.

Herrmann, K. (1976). Flavonols and flavones in food plants: a review. Int. J. Food Sci. Technol. **11:** 433–448.

Hirsch, C.N., et al. (2014). Insights into the maize pan-genome and pan-transcriptome. Plant Cell **26:** 121–135.

Ibrahim, R.K., Bruneau, A., and Bantignies, B. (1998). Plant *O*-methyltransferases: molecular analysis, common signature and classification. Plant Mol. Biol. **36:** 1–10.

Jander, G., Norris, S.R., Rounsley, S.D., Bush, D.F., Levin, I.M., and Last, R.L. (2002). Arabidopsis map-based cloning in the post-genome era. Plant Physiol. **129:** 440–450.

Jones, M.O., Piron-Prunier, F., Marcel, F., Piednoir-Barbeau, E., Alsadon, A.A., Wahb-Allah, M.A., Al-Doss, A.A., Bowler, C., Bramley, P.M., Fraser, P.D., and Bendahmane, A. (2012). Characterisation of alleles of tomato light signalling genes generated by TILLING. Phytochemistry **79:** 78–86.

Kang, J.H., Shi, F., Jones, A.D., Marks, M.D., and Howe, G.A. (2010a). Distortion of trichome morphology by the *hairless* mutation of tomato affects leaf surface chemistry. J. Exp. Bot. **61:** 1053–1064.

Kang, J.H., Liu, G., Shi, F., Jones, A.D., Beaudry, R.M., and Howe, G.A. (2010b). The tomato *odorless-2* mutant is defective in trichome-based production of diverse specialized metabolites and broad-spectrum resistance to insect herbivores. Plant Physiol. **154:** 262–272.

Kang, J.H., McRoberts, J., Shi, F., Moreno, J.E., Jones, A.D., and Howe, G.A. (2014). The flavonoid biosynthetic enzyme chalcone isomerase modulates terpenoid production in glandular trichomes of tomato. Plant Physiol. **164:** 1161–1174.

Kim, B.G., Lee, Y., Hur, H.G., Lim, Y., and Ahn, J.H. (2006). Flavonoid 3′-O-methyltransferase from rice: cDNA cloning, characterization and functional expression. Phytochemistry **67:** 387–394.

Kim, J., Kang, K., Gonzales-Vigil, E., Shi, F., Jones, A.D., Barry, C.S., and Last, R.L. (2012). Striking natural diversity in glandular trichome acylsugar composition is shaped by variation at the *Acyltransferase2* locus in the wild tomato *Solanum habrochaites.* Plant Physiol. **160:** 1854–1870.

Klein, T.W. (2005). Cannabinoid-based drugs as anti-inflammatory therapeutics. Nat. Rev. Immunol. **5:** 400–411.

Lam, K.C., Ibrahim, R.K., Behdad, B., and Dayanandan, S. (2007). Structure, function, and evolution of plant *O*-methyltransferases. Genome **50:** 1001–1013.

Lange, B.M., and Turner, G.W. (2013). Terpenoid biosynthesis in trichomes—current status and future opportunities. Plant Biotechnol. J. **11:** 2–22.

Last, R.L., Jones, A.D., and Shachar-Hill, Y. (2007). Towards the plant metabolome and beyond. Nat. Rev. Mol. Cell Biol. **8:** 167–174.

Li, C., Schmidt, A., Pichersky, E., Shi, F., and Jones, A.D. (2013). Identification of methylated flavonoid regioisomeric metabolites using enzymatic semisynthesis and liquid chromatography-tandem mass spectrometry. Metabolomics **9:** S92–S101.

Liu, B., Wang, H., Du, Z., Li, G., and Ye, H. (2011). Metabolic engineering of artemisinin biosynthesis in *Artemisia annua L.* Plant Cell Rep. **30:** 689–694.

Matsuba, Y., et al. (2013). Evolution of a complex locus for terpene biosynthesis in *solanum.* Plant Cell **25:** 2022–2036.

McCormick, S. (1991). Transformation of tomato with *Agrobacterium tumefaciens.* Plant Tissue Culture Manual **B6:** 1–9.

McDowell, E.T., et al. (2011). Comparative functional genomic analysis of Solanum glandular trichome types. Plant Physiol. **155:** 524–539.

Menda, N., Semel, Y., Peled, D., Eshed, Y., and Zamir, D. (2004). *In silico* screening of a saturated mutation library of tomato. Plant J. **38:** 861–872.

Morgante, M., De Paoli, E., and Radovic, S. (2007). Transposable elements and the plant pan-genomes. Curr. Opin. Plant Biol. **10:** 149–155.

Muzac, I., Wang, J., Anzellotti, D., Zhang, H., and Ibrahim, R.K. (2000). Functional expression of an Arabidopsis cDNA clone encoding a flavonol 3′-*O*-methyltransferase and characterization of the gene product. Arch. Biochem. Biophys. **375:** 385–388.

Ossowski, S., Schneeberger, K., Clark, R.M., Lanz, C., Warthmann, N., and Weigel, D. (2008). Sequencing of natural strains of *Arabidopsis thaliana* with short reads. Genome Res. **18:** 2024–2033.

Pichersky, E., and Lewinsohn, E. (2011). Convergent evolution in plant specialized metabolism. Annu. Rev. Plant Biol. **62:** 549–566.

Rodriguez, F., Wu, F., Ané, C., Tanksley, S., and Spooner, D.M. (2009). Do potatoes and tomatoes have a single evolutionary history, and what proportion of the genome supports this history? BMC Evol. Biol. **9:** 191.

Rodriguez-Saona, C., Vorsa, N., Singh, A.P., Johnson-Cicalese, J., Szendrei, Z., Mescher, M.C., and Frost, C.J. (2011). Tracing the history of plant traits under domestication in cranberries: potential consequences on anti-herbivore defences. J. Exp. Bot. **62:** 2633–2644.

Rounsley, S.D., and Last, R.L. (2010). Shotguns and SNPs: how fast and cheap sequencing is revolutionizing plant biology. Plant J. **61:** 922–927.

Saitou, N., and Nei, M. (1987). The neighbor-joining method: a new method for reconstructing phylogenetic trees. Mol. Biol. Evol. **4:** 406–425.

Sallaud, C., Giacalone, C., Topfer, R., Goepfert, S., Bakaher, N., Rosti, S., and Tissier, A. (2012). Characterization of two genes for the biosynthesis of the labdane diterpene *Z*-abienol in tobacco (*Nicotiana tabacum*) glandular trichomes. The Plant journal: for cell and molecular biology **72,** 1–17.

Sallaud, C., Rontein, D., Onillon, S., Jabès, F., Duffé, P., Giacalone, C., Thoraval, S., Escoffier, C., Herbette, G., Leonhardt, N., Causse, M., and Tissier, A. (2009). A novel pathway for sesquiterpene biosynthesis from *Z,Z*-farnesyl pyrophosphate in the wild tomato *Solanum habrochaites.* Plant Cell **21:** 301–317.

Schilmiller, A., Shi, F., Kim, J., Charbonneau, A.L., Holmes, D., Daniel Jones, A., and Last, R.L. (2010a). Mass spectrometry screening reveals widespread diversity in trichome specialized metabolites of tomato chromosomal substitution lines. Plant J. **62:** 391–403.

Schilmiller, A.L., Last, R.L., and Pichersky, E. (2008). Harnessing plant trichome biochemistry for the production of useful compounds. Plant J. **54:** 702–711.

Schilmiller, A.L., Pichersky, E., and Last, R.L. (2012a). Taming the hydra of specialized metabolism: how systems biology and

comparative approaches are revolutionizing plant biochemistry. Curr. Opin. Plant Biol. **15:** 338–344.

Schilmiller, A.L., Charbonneau, A.L., and Last, R.L. (2012b). Identification of a BAHD acetyltransferase that produces protective acyl sugars in tomato trichomes. Proc. Natl. Acad. Sci. USA **109:** 16377–16382.

Schilmiller, A.L., Miner, D.P., Larson, M., McDowell, E., Gang, D.R., Wilkerson, C., and Last, R.L. (2010b). Studies of a biochemical factory: tomato trichome deep expressed sequence tag sequencing and proteomics. Plant Physiol. **153:** 1212–1223.

Schilmiller, A.L., Schauvinhold, I., Larson, M., Xu, R., Charbonneau, A.L., Schmidt, A., Wilkerson, C., Last, R.L., and Pichersky, E. (2009). Monoterpenes in the glandular trichomes of tomato are synthesized from a neryl diphosphate precursor rather than geranyl diphosphate. Proc. Natl. Acad. Sci. USA **106:** 10865–10870.

Schmidt, A., Li, C., Jones, A.D., and Pichersky, E. (2012). Characterization of a flavonol 3-*O*-methyltransferase in the trichomes of the wild tomato species *Solanum habrochaites.* Planta **236:** 839–849.

Schmidt, A., Li, C., Shi, F., Jones, A.D., and Pichersky, E. (2011). Polymethylated myricetin in trichomes of the wild tomato species *Solanum habrochaites* and characterization of trichome-specific 3′/5′- and 7/4′-myricetin *O*-methyltransferases. Plant Physiol. **155:** 1999–2009.

Schneeberger, K., et al. (2011). Reference-guided assembly of four diverse *Arabidopsis thaliana* genomes. Proc. Natl. Acad. Sci. USA **108:** 10249–10254.

Somerville, C., and Somerville, S. (1999). Plant functional genomics. Science **285:** 380–383.

Springer, N.M., et al. (2009). Maize inbreds exhibit high levels of copy number variation (CNV) and presence/absence variation (PAV) in genome content. PLoS Genet. **5:** e1000734.

Stevens, J., Hart, H., and Wollenweber, E. (1995). The systematic and evolutionary significance of exudate flavonoids in Aeonium. Phytochemistry **39:** 805–813.

Swanson-Wagner, R.A., Eichten, S.R., Kumari, S., Tiffin, P., Stein, J.C., Ware, D., and Springer, N.M. (2010). Pervasive gene content variation and copy number variation in maize and its undomesticated progenitor. Genome Res. **20:** 1689–1699.

Tamura, K., Peterson, D., Peterson, N., Stecher, G., Nei, M., and Kumar, S. (2011). MEGA5: Molecular Evolutionary Genetics Analysis using maximum likelihood, evolutionary distance, and maximum parsimony methods. Mol. Biol. Evol.

Thompson, J.D., Higgins, D.G., and Gibson, T.J. (1994). CLUSTAL W: improving the sensitivity of progressive multiple sequence alignment through sequence weighting, position-specific gap penalties and weight matrix choice. Nucleic Acids Res. **22:** 4673–4680.

Tomato Genome Consortium (2012). The tomato genome sequence provides insights into fleshy fruit evolution. Nature **485:** 635–641.

Tissier, A. (2012). Glandular trichomes: what comes after expressed sequence tags? The Plant journal: for cell and molecular biology **70,** 51–68.

Wagner, G.J. (1991). Secreting glandular trichomes: more than just hairs. Plant Physiol. **96:** 675–679.

Wang, G., Tian, L., Aziz, N., Broun, P., Dai, X., He, J., King, A., Zhao, P.X., and Dixon, R.A. (2008). Terpene biosynthesis in glandular trichomes of hop. Plant Physiol. **148:** 1254–1266.

Weigel, D., and Mott, R. (2009). The 1001 genomes project for *Arabidopsis thaliana.* Genome Biol. **10:** 107.

Weinhold, A., and Baldwin, I.T. (2011). Trichome-derived *O*-acyl sugars are a first meal for caterpillars that tags them for predation. Proc. Natl. Acad. Sci. USA **108:** 7855–7859.

Winzer, T., et al. (2012). A *Papaver somniferum* 10-gene cluster for synthesis of the anticancer alkaloid noscapine. Science **336:** 1704–1708.

Yifhar, T., Pekker, I., Peled, D., Friedlander, G., Pistunov, A., Sabban, M., Wachsman, G., Alvarez, J.P., Amsellem, Z., and Eshed, Y. (2012). Failure of the tomato trans-acting short interfering RNA program to regulate *AUXIN RESPONSE FACTOR3* and *ARF4* underlies the wiry leaf syndrome. Plant Cell **24:** 3575–3589.

Analysis of Natural and Induced Variation in Tomato Glandular Trichome Flavonoids Identifies a Gene Not Present in the Reference Genome

Jeongwoon Kim, Yuki Matsuba, Jing Ning, Anthony L. Schilmiller, Dagan Hammar, A. Daniel Jones, Eran Pichersky and Robert L. Last

Plant Cell 2014;26;3272-3285; originally published online August 15, 2014;
DOI 10.1105/tpc.114.129460